Optimisation, Simulation, and Characterisation of Mahogany (*Khaya Senegalensis*) Seed Oil Extract

Dauda Baba [1, 2], **Umar Omeiza Aroke** [2], **Jibril Mohammed** [2], **Saidat Olanipekun Giwa** [2]

[1] *University of Maiduguri*
Along Bama Road, Maiduguri, Borno State, Nigeria

[2] *Abubakar Tafawa Balewa University*
Dass road, P. M. B. 0248, Bauchi, 740272, Nigeria

DOI: 10.22178/pos.107-50

LCC Subject Category: T1-995

Received 30.07.2024
Accepted 25.08.2024
Published online 31.08.2024

Corresponding Author:
Dauda Baba
dbaba@unimaid.edu.ng

© 2024 The Authors. This article is licensed under a Creative Commons Attribution 4.0 License

Abstract. The increasing demand for sustainable biofuel alternatives has encouraged the exploration of non-edible seed oils, with mahogany (*Khaya Senegalensis*) seed oil emerging as a promising candidate. This study investigates the optimisation of oil extraction from mahogany seeds using a combined response surface methodology (RSM) approach and process simulation. Soxhlet extraction with n-hexane as the solvent was employed, and the effects of extraction time, temperature, solvent/seed ratio, and particle size on oil yield were evaluated. A central composite rotatable design (CCRD) was used to develop a statistically significant model that accurately predicted oil yield based on the selected process parameters. Optimisation through RSM identified the optimal extraction conditions as 106 minutes extraction time, 68°C temperature, 5.05 ml/g solvent/seed ratio, and particle size of 1 mm. These conditions resulted in a maximum experimental oil yield of 58.9%, which agreed with the model's prediction of 61.17%. The extracted oil was characterised using gas chromatography-mass spectrometry (GC-MS) and Fourier transform infrared spectroscopy (FTIR). The analysis revealed a high content of unsaturated fatty acids, primarily linoleic acid (38.93%) and oleic acid (24.43%); other minor components, such as palmitic acid (0.34%) and stearic acid (2.74%), were also present making it suitable for biodiesel production.

Furthermore, an Aspen Plus® model was developed to simulate the entire extraction process, including purification and solvent recovery. Sensitivity analysis and optimisation of the model led to 99.99% oil purity and complete hexane recovery, demonstrating the potential for sustainable and efficient oil extraction for the biodiesel production process. This study highlights the efficacy of combining experimental optimisation through RSM with process simulation for maximising oil yield and achieving high-quality oil suitable for biodiesel production.

Keywords: Characterisation; mahogany seed; optimisation; response surface methodology; simulation; solvent extraction.

INTRODUCTION

Mahogany (*Khaya Senegalensis*), belonging to the family Meliaceae, is a multipurpose tree that grows to 30 m in height and has a diameter of up to 1.5 meters. There are distinctive round capsules with woody fruits on this evergreen tree, with a round crown of dark shiny foliage, pinnate leaves, and a characteristic evergreen crown. Four to five valves are embedded in the fruit, which has a 4-6 cm diameter and several seeds ranging from 6 to 18. It produces seeds resembling flat disks, each 2-3.6 cm long, weighing 289 g per 1000 seeds [1]. The oil extracted from mahogany seeds is non-edible but holds promise as a sustainable feedstock for biodiesel production [2]. However, efficient extraction methods are crucial for economic viability. Optimising the ex-

traction of non-edible oils like mahogany seed oil is essential for biodiesel production. This optimisation has two key aspects: 1) Refining existing extraction techniques to achieve the highest possible oil yield, and 2) Creating a model of the extraction process that can guide optimisation efforts and facilitate scaling up for commercial biodiesel production.

Response Surface Methodology (RSM) is a powerful statistical tool for optimising various processes, including oil extraction. RSM allows for evaluating how multiple factors (e.g., solvent type, temperature, extraction time, particle size) interact and influence the response variable (e.g., oil yield). By conducting designed experiments and statistically analysing the data, RSM helps develop a mathematical model that predicts oil yield based on the chosen factors [3]. This model aids in identifying the optimal combination of parameters to maximise oil extraction efficiency. However, RSM primarily focuses on experimental design and optimisation within a laboratory setting. Aspen Plus, a process simulation software, complements RSM by providing a virtual model of the actual extraction process, specifically the Soxhlet extraction for mahogany seed oil [4]. Analysing these balances provides a deeper understanding of how various factors impact oil yield, ultimately aiding in optimising process parameters for commercial applications. This combined approach paves the way for developing more robust strategies to maximise oil yield, a critical step towards efficient and sustainable biodiesel production.

Several studies have investigated the potential of Mahogany seeds for biodiesel production. Authors [5] characterised the fatty acid composition of the oil using Soxhlet extraction, while [6] focused on isolating and characterising the oil through n-hexane solvent extraction. While these studies provide valuable information on the oil's properties, they don't address optimising oil yield or quality. Similarly, authors [2] compared the oil yield from mahogany seeds using mechanical pressing with results from other species, but optimisation was not a primary focus. There appears to be a gap in the literature regarding a dedicated and systematic study on optimising the extraction process for Mahogany seeds. This study addresses this gap by presenting a comprehensive investigation on optimising oil extraction from mahogany seeds to maximise oil yield.

METHODOLOGY

Mahogany seeds (MS) were collected from mature Mahogany trees in Maiduguri, Borno State, Nigeria. All chemicals used in this study were analytical grade and purchased from a commercial supplier. These included n-hexane, potassium hydroxide (KOH), ethanol (95%), hydrochloric acid (HCl), and phenolphthalein.

Seed Preparation. This study adapted a method [7] to prepare mahogany seed (MS). MS seeds were sun-dried on open trays for three days to ensure uniform drying with regular turning. Drying occurred during the dry season (April-June), with approximately 6-8 hours of direct sunlight exposure daily. Next, the dried seeds were ground into a fine powder using an electric blender (SHB-3088). To obtain two distinct particle size fractions, the ground powder was sieved using British Standard Sieves (BSS) with mesh sizes of 2 mm (No. 8) and 1 mm (No. 16). This resulted in a coarse fraction with particles less than 2 mm; a fine fraction with particles less than 1 mm.

Both sieved fractions underwent further drying in a hot air oven (Kalstein, YR05264 (A)) at 60°C for 2 hours to eliminate residual moisture. Finally, the dried seed fractions were stored in airtight containers at room temperature.

Experimental Design. A central composite rotatable design (CCRD) was employed because it can efficiently explore the quadratic response surface and estimate both linear and interaction effects of independent variables on the response [8]. This statistical approach allows for the optimisation of multiple parameters simultaneously while minimising the number of experimental runs required [9]. Design-Expert® 13.0.0 software (Stat-Ease Inc., Minneapolis, MN, USA) was utilised to generate the experimental design and analyse the resulting data.

Four independent variables influencing oil yield were selected based on previous studies [7, 10]. The specific ranges for each variable are detailed in Table 1.

The primary response variable of interest in this investigation was oil yield, expressed as a percentage. The calculation of oil yield (%) followed Equation 1 outlined [7].

Table 1 – Independent Variables and Levels with Coded and Natural Values used in the Central Composite Rotatable Designs (CCRD) of the Oil Extraction Experiment

Factor	Unit	Symbol	Coded Variable (Ranges)	
			-α (lower)	α (Upper)
Time	minutes	A	40	120
Temperature	°C	B	60	80
Solvent / solid ratio	ml/g	C	3	6
Particle Size	mm	D	1	2

Extraction and Separation Process. Oil extraction was performed using a Soxhlet extraction apparatus consisting of a 250 ml glass extraction chamber, a 500 ml round bottom flask, and a condenser. For each extraction run, a 10 g sample of Mahogany seed powder with a specific particle size (either 2 mm or 1 mm based on the experimental design matrix) was weighed accurately and placed into a cellulose thimble (Whatman, 30 x 100 mm). The thimble was then stapled to prevent any loss of seed powder during the extraction process. A predetermined volume of the solvent, n-hexane (based on the experimental design matrix, Table 2), was added to the round bottom flask. The flask was then placed on a heating mantle with a temperature controller and magnetic stirrer. The condenser was connected to a chiller to ensure efficient cooling and prevent solvent loss. The extraction was done by heating the solvent to its boiling point, allowing it to vaporise and condense in the condenser, dripping down onto the seed powder in the thimble. The extraction cycle was continued for a specific time per the experimental design matrix. After the extraction, the solvent was evaporated from the oil-solvent mixture at a temperature of 60°C. The extracted oil was then collected and weighed to determine the oil yield using Equation 1 [7].

$$Oil\ yield,\ \% = \frac{Weight\ of\ oil\ obtained}{Weight\ of\ seeds\ powder\ used\ for\ extraction} \times 100 \quad (1)$$

Physicochemical Properties of the Oil. Moisture content. The moisture content of the extracted oil was determined using the American Oil Chemists' Society (AOCS) [11]. Approximately 5 grams of oil sample was weighed accurately into a pre-dried and tared aluminium dish. The dish was placed in a hot air oven (Kalstein, YR05264 (A)) at 105°C for 3 hours. After drying, the dish was cooled in a desiccator and weighed again. The moisture content was calculated as the percentage weight loss of the sample using Equation (2).

$$Moisture\ content\ (\%) = \frac{Original\ Weight\ of\ sample - weight\ of\ sample\ after\ drying}{Original\ Weight\ of\ sample} \times 100 \quad (2)$$

Physicochemical Properties of the Oil. Determination of the Relative Density. The relative density of the extracted oil was determined according to the ASTM D1298-12b standard test method [12] using a hydrometer. The oil sample was brought to a temperature of 30°C and carefully transferred to a hydrometer cylinder pre-equilibrated to the same temperature. A calibrated hydrometer, also at the same temperature, was gently lowered into the oil and allowed to settle freely. After reaching thermal equilibrium, the hydrometer scale reading and the oil temperature were recorded. The observed hydrometer reading was then corrected to the reference temperature petroleum measurement tables. The specific gravity and density were calculated using Equation 3 and 4 [13].

$$Specific\ gravity = \frac{Weight\ of\ 50\ \text{ml of oil}}{Weight\ of\ 50\ mL\ of\ water} \quad (3)$$

$$Density\ (g/l) = \frac{Weight\ of\ 50\ \text{ml of oil}}{Volume\ of\ 50\ mL\ of\ oil} \quad (4)$$

Physicochemical Properties of the Oil. Dynamic Viscosity. The dynamic viscosity of the extracted oil was determined using a Brookfield Digital rotational viscometer (Middleboro, MA02346) according to the ASTM D445 standard test method [14]. The oil sample was preheated to 40°C in a temperature-controlled water bath. A suitable spindle was selected based on the expected viscosity range of the oil. The spindle was then immersed into the oil sample, ensuring proper alignment and depth. The viscometer was set to the appropriate rotational speed, and the measurement was initiated. The dynamic viscosity reading and the operating temperature were displayed on the viscometer screen and recorded in millipascal-second units (mPa·s).

Physicochemical Properties of the Oil. Kinematic Viscosity. The kinematic viscosity of the oil was

calculated by dividing the measured dynamic viscosity by the density of the oil at the same temperature [14], as shown in Equation 5:

$$Kinematic\ viscosity\ (\vartheta) = \frac{Dynamic\ viscosity\ of\ the\ Oil}{Density\ of\ the\ Oil} \quad (5)$$

Physicochemical Properties of the Oil. Acid Value and Free Fatty Acid (FFA) Determination. The acid value of the extracted oil was determined according to the standard test method [15], which describes a potentiometric or colourimetric titration method. This standardised method ensures consistent and reliable measurement of acidity in fats and oils across laboratories. Approximately 0.5 grams of the oil sample was accurately weighed using an analytical balance to minimise errors associated with mass measurement. The sample was then transferred to a 250 ml Erlenmeyer flask for titration. Neutralised ethanol-diethyl ether (1:1 v/v) solution (50 ml) was added to the flask. This solvent mixture effectively dissolves the oil sample while remaining neutral, preventing interference with the acid-base titration. The mixture was gently heated on a hot plate with continuous swirling to facilitate the complete dissolution of the oil sample. A few drops of phenolphthalein indicator solution were added to the solution. Phenolphthalein is a weak acid-base indicator that changes colour from colourless (acidic) to pale pink (primary) at the endpoint of the titration. The solution was titrated with a standardised 0.1 M potassium hydroxide (KOH) solution. The burette allows precise and controlled addition of the KOH solution during the titration. The endpoint of the titration was reached when a pale pink colour persisted for at least 30 seconds, indicating complete neutralisation of the free fatty acids in the oil sample by the KOH solution. The acid value (mg KOH/g oil) and free fatty acid (FFA) content (%) of the oil were calculated using equations (6) and (7), respectively, as described in the referenced ASTM standard [15]. These equations consider the volume of KOH solution used, its molarity, the molecular weight of KOH, and the weight of the oil sample to determine the acid content and the corresponding FFA content.

$$Acid\ Value\ (mg\ KOH/g\ oil) = \frac{\text{volume (mL) of 0.1 M KOH used} \times \text{molarity of the KOH} \times 56.1}{\text{weight of the oil sample}} \quad (6)$$

$$FFA\ Content\ (\%) = \frac{Acid\ value}{2} \quad (7)$$

Process Simulation. A process model for Mahogany seed oil extraction was developed using Aspen Plus® V12.1 software to simulate the critical unit operations and analyse process parameters. The model aimed to evaluate the efficiency of the extraction process, optimise solvent recovery, and provide insights for potential scale-up.

The Mahogany seed, a complex solid material, was modelled as a non-conventional component using the SOLIDS model in Aspen Plus®. The seed composition was defined based on the USDA nutritional database, with the fat content (39.5%) being the primary focus of the simulation. The fatty acid profile obtained from the GC-MS analysis was used to define the composition of the extracted oil, including oleic acid (28%), linoleic acid (48%), stearic acid (3%) and other minor fatty acid components. N-hexane was chosen as the solvent for the extraction process due to its effectiveness in extracting non-polar lipids. The Peng-Robinson-Boston-Mathias (PR-BM) equation of state was used to model the thermodynamic properties of the conventional components (solvent and fatty acids) due to its suitability for mixtures involving hydrocarbons and polar compounds.

The process flowsheet (Figure 1) consisted of four main stages: feed preparation, drying, extraction, and separation.

A mixer unit (MIX-1) was used to combine the Mahogany seed powder (M-SEED) with air (AIR-1) at ambient temperature. To simulate atmospheric conditions, the air stream comprised 79% nitrogen (N2) and 21% oxygen (O2). A rotary dryer unit (DRYER) removed moisture from the seed. The dryer was operated at a temperature of 60°C and a pressure of 1 atm. The dried seed stream (DRY-SEED) exited the dryer with less than 5% moisture content.

The SWASH unit simulated the solid-liquid extraction process with n-hexane as the solvent. A RadFrac distillation column (DIST) separated the extracted oil from the solvent. The column was configured with 25 equilibrium stages and a partial condenser. The recovered hexane (SOL-REC) was recycled back to the extraction stage.

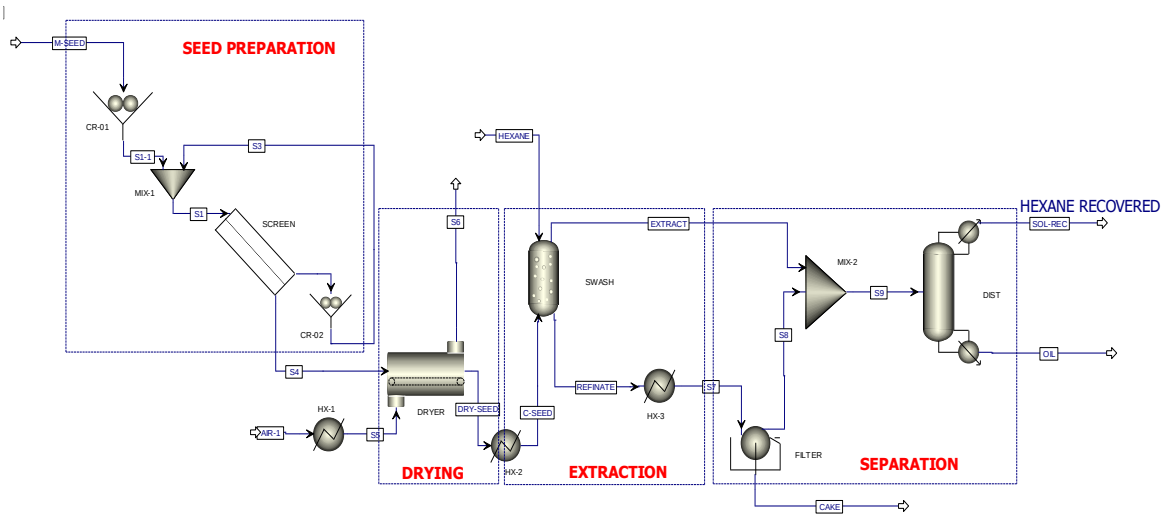

Figure 1 – Process Flow Diagram of the Oil Extraction from Mahogany Seed

RESULTS AND DISCUSSION

Optimisation of Extraction Conditions. The results of 34 experimental runs conducted using a central composite rotatable design (CCRD) to optimise the extraction of mahogany seed oil are presented in Table 2.

Table 2 – Experimental Responses for the Mahogany Oil Extraction

Run	Independent variables				Responses	
	A: Time (min)	B: Temperature (oC)	C: Solvent/Solid (mL/g)	D: Particle Size (mm)	Actual yield (%)	Predicted yield (%)
1	40	70	4.5	1	33.20	32.26
2	104	76	3.6	2	36.10	37.33
3	56	64	5.4	1	24.40	25.23
4	104	64	5.4	2	34.10	33.88
5	56	64	3.6	1	47.40	47.04
6	56	64	5.4	2	50.70	50.26
7	104	64	3.6	1	31.40	30.83
8	80	70	3.0	1	52.20	54.84
9	104	76	3.6	1	45.30	43.93
10	56	76	3.6	1	40.00	38.85
11	80	60	4.5	1	38.00	38.74
12	104	76	5.4	2	44.80	44.84
13	80	80	4.5	2	38.60	38.29
14	56	76	5.4	1	46.70	46.73
15	80	70	4.5	1	47.30	43.64
16	56	76	5.4	2	37.30	37.13
17	120	70	4.5	2	39.10	39.36
18	80	60	4.5	2	37.40	37.71
19	80	70	3.0	2	47.00	45.09
20	80	80	4.5	1	45.90	48.54
21	80	70	4.5	2	38.20	38.00
22	56	64	3.6	2	26.30	27.05
23	56	76	3.6	2	27.60	28.61
24	104	64	3.6	2	34.40	35.34
25	40	70	4.5	2	29.10	29.88
26	80	70	6.0	2	30.00	30.91
27	104	76	5.4	1	52.10	51.92
28	80	70	4.5	1	43.00	43.64

Run	Independent variables				Responses	
29	80	70	6.0	1	32.60	32.44
30	120	70	4.5	1	48.70	48.26
31	80	70	4.5	2	37.50	38.00
32	104	64	5.4	1	54.40	55.01
33	80	70	4.5	2	41.50	38.00
34	80	70	4.5	1	43.00	43.64

The factors investigated were extraction time (A), extraction temperature (B), solvent/solid ratio (C), and particle size (D). The response variable was the oil yield (%), which represents the percentage of oil extracted from the seeds under each set of conditions. In addition, Table 2 shows the actual oil yield (%) obtained for each experimental run, along with the corresponding predicted yield (%) generated by the RSM model. The observed oil yield ranged from 24.4% to 54.4%, highlighting the significant influence of the selected process parameters on the extraction efficiency. The model's accuracy in predicting the yield can be assessed by comparing the actual and predicted values. Although the model doesn't predict the yield perfectly in every run, it demonstrates good overall accuracy, particularly for specific runs. This suggests the model could help guide further optimisation.

The experimental data was fitted to various polynomial models using Design-Expert software. Linear, quadratic and cubic models were initially explored but yielded unsatisfactory results. Consequently, a reduced quartic model was chosen to capture the potential non-linear relationships between the factors and oil yield. This model was further refined by removing statistically insignificant terms (aliased and non-hierarchical) to improve its overall significance. The resulting empirical models, expressed in actual terms for 1 mm and 2 mm particle sizes, are presented in Equations (7) and Equation (8), respectively.

For Particle size: 1 mm

$$Y_{1\,mm}(\%) = 803.41049 - 0.78169A - 17.08383B - 192.81894C + 0.20178AB + 0.62123AC + 3.95719BC - 0.09917A^2 - 0.04549ABC + 0.01772A^2C + 0.00007A^3$$

For Particle size: 2 mm

$$Y_{2\,mm} = -1070.46333 + 21.03615A + 7.34672B + 261.57845C - 0.08388AB - 4.62792AC - 2.01163BC - 0.099173A^2 + 0.02346ABC + 0.017716A^2C + 0.00007A^3$$

where Y1 mm and Y2 mm = Oil yield for 1 mm and 2 mm particle size, respectively.

The analysis of variance (ANOVA) results, presented in Table 3, offer valuable insights into the influence of various factors on oil yield from mahogany seeds using a solvent-based method.

Table 3 – Analysis of Variance (ANOVA) for the Reduced Cubic Model of Mahogany Oil Yield

Source	Sum of Squares	df	Mean Square	F-value	p-value	
Model	2032.97	18	112.94	29.81	< 0.0001	significant
A-Time	6.14	1	6.14	1.62	0.2223	
B-Temperature	65.05	1	65.05	17.17	0.0009	
C-Solvent/Solid	334.52	1	334.52	88.29	< 0.0001	
D-Particle Size	270.21	1	270.21	71.31	< 0.0001	
AB	28.17	1	28.17	7.43	0.0156	
AC	26.04	1	26.04	6.87	0.0193	
AD	25.6	1	25.6	6.76	0.0201	
BC	3.77	1	3.77	0.9958	0.3342	
BD	51.36	1	51.36	13.55	0.0022	
CD	40.72	1	40.72	10.75	0.0051	

Source	Sum of Squares	df	Mean Square	F-value	p-value	
A^2	37.24	1	37.24	9.83	0.0068	
ABC	30.89	1	30.89	8.15	0.012	
ABD	48.41	1	48.41	12.78	0.0028	
ACD	322.11	1	322.11	85.01	< 0.0001	
BCD	23.11	1	23.11	6.1	0.026	
A^2C	529.48	1	529.48	139.74	< 0.0001	
A^3	20.93	1	20.93	5.52	0.0329	
ABCD	302.5	1	302.5	79.83	< 0.0001	
Residual	56.84	15	3.79			
Lack of Fit	35.21	11	3.2	0.5921	0.7779	not significant
Pure Error	21.63	4	5.41			
Cor Total	2089.8	33				
Std. Dev.	1.95		R^2	0.9728		
Mean	39.86		Adjusted R^2	0.9402		
CV %	4.88		Predicted R^2	0.8029		
			Adeq Precision	20.4688		

This information is critical for identifying the optimal conditions for maximising extraction efficiency. The ANOVA revealed a complex interaction between the independent variables and oil yield. Statistically significant positive effects (p-value < 0.05) were observed for extraction temperature (p = 0.0009), solvent/solid ratio (p < 0.0001), and particle size (p = 0.0001). This suggests that increasing these factors generally led to higher oil yields within the studied range.

However, reaction time displayed a p-value of 0.2223, more significant than 0.05. Therefore, insufficient statistical evidence exists to conclude that reaction time significantly impacts oil yield within the tested range. This information optimises the solvent-based extraction process by focusing on parameters with a statistically proven influence on oil yield. Even if time itself is not significant, it might still have a significant interaction (P-value < 0.05) with other factors, as indicated by the ANOVA results for the interaction terms AB, AC, AD, A^2, ABC, ABD, ACD, A^2C, A^3 and ABCD. Other significant interactions include BC, BD, CD and BCD with p-values < 0.05.

Since the F-value is a ratio that compares the variance explained by the model to the unexplained variance, the high F-value (29.81) and very low p-value (< 0.0001) indicate a statistically significant model fit, suggesting that the model adequately represents the relationship between the independent variables and the response variable (oil yield). The lack of fit P-value (0.0962) is above the commonly used significance level of 0.05. This indicates that the data does not provide strong enough evidence to reject the null hypothesis (the null hypothesis of the Lack of Fit test states that there is no lack of fit, meaning the chosen model is sufficient to describe the data.). Therefore, there is no significant lack of fit (Table 3), meaning the model adequately captures the relationship between the independent variables and oil yield. The developed model exhibited a good fit (R^2 = 0.9728) and strong predictive ability within the investigated range (adjusted R^2 = 0.9402). However, the difference between R^2 and adjusted R^2 suggests potential overfitting. While the moderate predicted R^2 (0.8229) is still acceptable, the model's prediction accuracy might decrease for data points outside the experimental conditions. This highlights the limitations of extrapolating the model's effectiveness beyond the studied range of factors (e.g., temperature, solvent ratio). Further validation with additional data points and potentially a more comprehensive range of experimental parameters might be necessary to improve the model's generalizability and ensure its accuracy for broader operating conditions.

Interaction of extraction time and temperature. Figure 2 illustrates the interactive effects of extraction time (A) and temperature (B) on oil yield.

Both factors positively affect yield, but temperature shows greater sensitivity, particularly below 70°C, where small changes result in substantial yield differences. Within the optimal temperature range, increasing extraction time generally results in higher yields, as evidenced by the upward trend of the contour lines and the rising surface of the 3D plot.

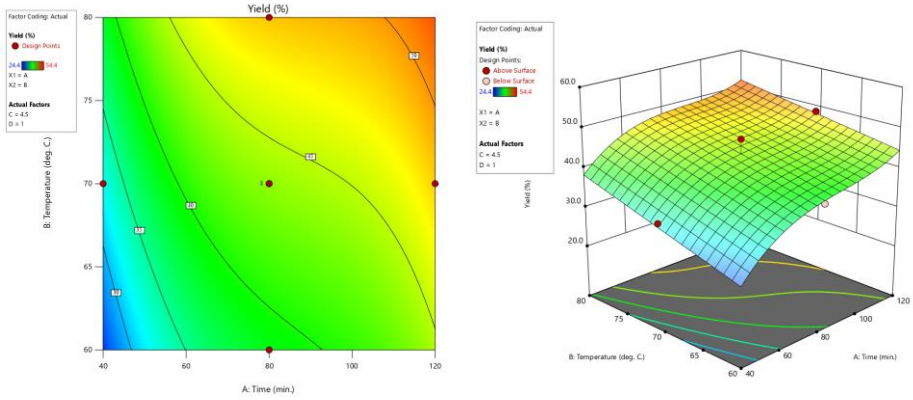

Figure 2 – Contour Plot (Left) and 3D Surface Plot (Right) Showing the Effect of Time and Temperature on the Oil Yield

However, diminishing returns are observed with time; the rate of yield increase slows down beyond a certain point, as evidenced by the more expansive space between the contour lines as time increases, indicating a limit to the extractable oil, even with prolonged solvent contact. In general, temperature appears to be a more critical factor than time over the range studied, highlighting the importance of optimising both factors to achieve maximum oil yield.

Interaction of extraction time and solvent/solid ratio. Figure 3 shows the interactive effects of extraction time (A) and solvent/solid ratio (C) on oil yield while holding temperature (B) and particle size (D) constant.

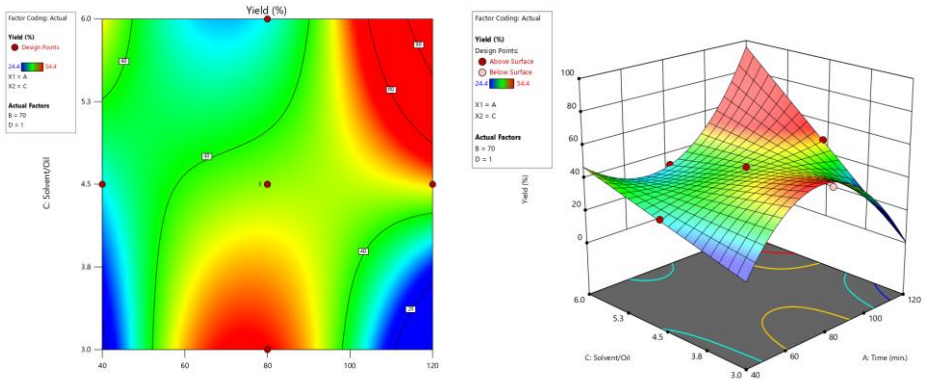

Figure 3 – Contour Plot (Left) and 3D Surface plot (Right) Showing the effect of time and temperature on the oil yield

Optimal yields, represented by the red and orange regions in the contour plot, cluster around a solvent/solid ratio of 4.5 to 6 and extraction times of 80 to 120 minutes. The contour plot shows that increasing extraction time generally increases yield up to a certain point, after which further increases result in diminishing returns as indicated by the plateauing or slight decrease in yield. Similarly, there is an optimum range for the solvent/solid ratio, with yields decreasing at very low and very high ratios. The curved contour lines emphasise the significant interaction between time and solvent/solid ratio, highlighting that their combined influence determines the final oil yield.

Interaction of extraction temperature and solvent/solid ratio. The relationship between extraction temperature (B), solvent/solid ratio (C), and oil yield, keeping extraction time (A) and particle size (D) constant is illustrated in Figure 4.

The 3D surface and 2D contour plots indicate that the highest oil yields (represented by the red/orange areas) are obtained at moderate to high temperatures (around 70-75 °C) and a solvent/solid ratio between approximately 4.5 and 5.5.

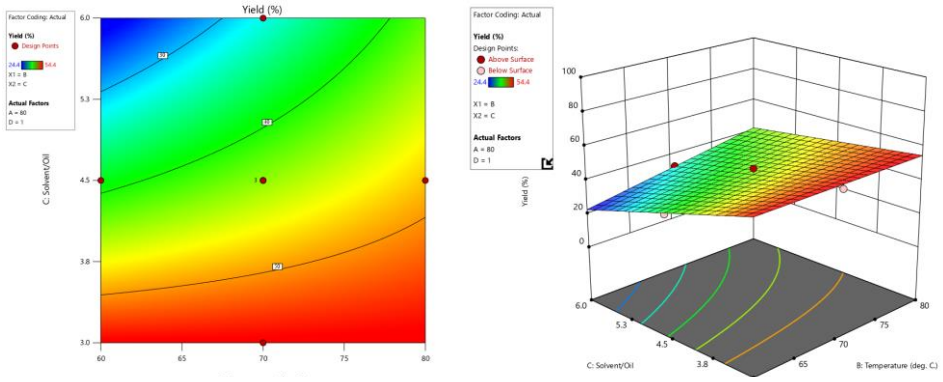

Figure 4 – Contour Plot (Left) and 3D Surface plot (Right) Showing the Effect of Time and Temperature on the Oil Yield

The contour lines are closely spaced in the lower temperature range (below 70°C), indicating a steep change in yield with slight temperature variations. This suggests that the extraction process is susceptible to temperature in this region. The contour lines become more widely spaced at higher solvent/solid ratios, suggesting that increasing the ratio beyond a certain point (around 5.5) does not significantly improve yield. The curved shape of the contour lines indicates an interaction between temperature and solvent/solid ratio. The optimal solvent/solid ratio for maximum yield appears to shift slightly towards higher values as the temperature increases.

Interaction of particle size and extraction time. Figure 5 explores the impact of extraction time (A) and particle size (D) on oil yield. It clearly shows that particle size significantly influences oil yield.

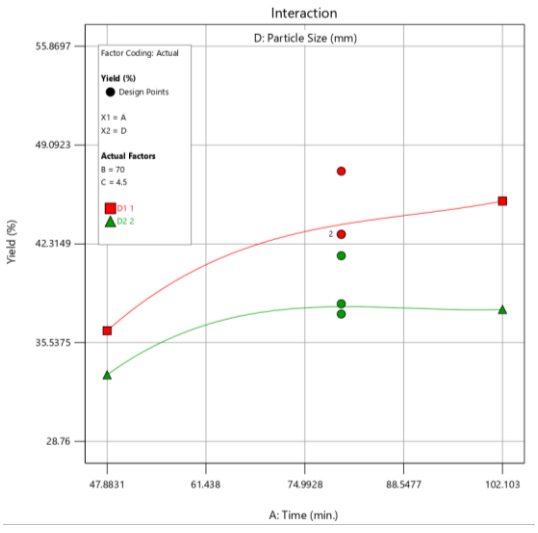

Figure 5 – The effect of time and particle size on the oil yield

Smaller particle sizes (D1 = 1mm, red lines) consistently yield higher yields than larger particle sizes (D2 = 2mm, green lines) across all tested extraction times. This is justified as smaller particles have a larger surface area exposed to the solvent, allowing for faster and more efficient oil extraction. For both particle sizes, yield generally increases with longer extraction times but with diminishing returns, especially for the smaller particle size (D1). The lines begin to plateau as extraction time increases, suggesting that extending the process doesn't substantially improve yield beyond a certain point. The non-parallel lines indicate an interaction between particle size and extraction time. The impact of extraction time is more pronounced for smaller particle sizes (D1). This means the benefit of more prolonged extraction is more remarkable when using smaller particles. Therefore, a smaller particle size (D1) is strongly recommended for maximum oil yield. While longer extraction times also contribute to higher yield, the optimal time should be determined considering the trade-off between yield improvement and processing costs (time and energy).

Interaction of particle size and extraction temperature. Figure 6 illustrates the effect of the interaction between particle size (D) and temperature (B) on oil yield. The two lines representing different particle sizes (D1 = 1 mm and D2 = 2 mm) are not parallel, indicating an interaction effect between particle size and temperature. At lower temperatures (below 60°C), particle size has a negligible effect on yield.

Hence, both D1 and D2 yield similar results. As temperature increases, the difference in yield between the two particle sizes becomes more pronounced.

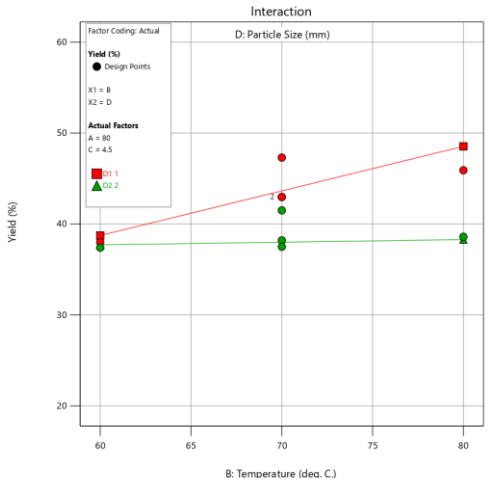

Figure 6 – The effect of temperature and particle size on the oil yield

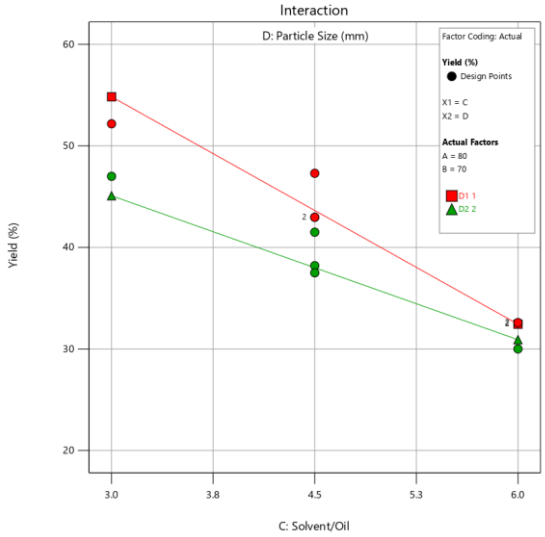

Figure 7 – The effect of solvent/solid ratio and particle size on the oil yield

Smaller particle sizes (D1, the red line) show a steeper upward trend than larger particles (D2, the green line). This is evidenced by smaller particles having a larger surface area-to-volume ratio, exposing more of the internal matrix containing the target compounds to the solvent. This increased surface area facilitates faster mass transfer rates, allowing more oil to be extracted, especially as temperature increases and further enhances the diffusion and solubility of the oil. While larger particles, with their lower surface area, have limited mass transfer rates. Even at higher temperatures, extraction from the core of these particles might be hindered. The diverging pattern indicates that the effect of temperature on oil yield depends on the particle size:

- Smaller Particles (D1): Benefit more from higher temperatures, exhibiting a more significant increase in yield.

- Larger Particles (D2): Show a less pronounced increase in yield with rising temperatures.

This interaction effect highlights the importance of considering particle size and temperature when optimising extraction processes.

Interaction of particle size and extraction temperature. Figure 7 illustrates the effect of the interaction between particle size (D) and solvent/solid ratio (C) on oil yield while holding time (A) and temperature (B) constant.

The smaller particle size (D1 = 1 mm, the red line) and the larger particle size (D2 = 2 mm, the green line) are not parallel, which implies an interaction effect between particle size and the solvent/solid ratio.

Both particle sizes show a general decrease in oil yield as the solvent/solid ratio increases. This is because the solvent becomes increasingly saturated with the extracted oil. This saturation effect limits further extraction, leading to the decreasing trend observed for both particle sizes. At higher solvent/oil ratios, the difference in yield between the two particle sizes is minimal. This interaction plot reveals that the effect of solvent/oil ratio on yield is not independent but is influenced by particle size. This shows an essential implication for process design. For instance, if grinding to smaller sizes is not economically feasible, adjusting the solvent/oil ratio might compensate somewhat, especially at the early stages of extraction when the solvent is not yet saturated.

After determining the statistical significance of the model, an optimisation process was conducted based on experimental results in Table 2 and the observation inferred from the contour and 3D surface plots. The highest oil yields for 1 mm and ≤ 2 mm particle sizes were 54.4 % and 50.70 %, respectively. The particle size interaction from Figures 5 through 7 also confirmed that smaller particle size (D1 = 1 mm) is more favourable regarding higher yield. The condition of the factors at this higher yield (54.4 %) is 115 min, 64°C, solvent/solid ratio of 5.4 and particle size of 1 mm. These values were the target operating conditions for the optimisation process, which predicted maximum yields of 61.17 % with desirability of 1 at 106 min, 68 °C, solvent/solid ratio of 5.05 and particle size of 1 mm. A confirmation experiment was performed at this condition

and obtained a maximum yield of 58.9 %, close to the predicted value.

Table 4 compares the yield obtained in this study with yields reported in the literature for other oilseed crops using similar solvent extraction methods.

Table 4 – Comparison of Oil Extraction Yields from Different Oilseed Crops

Plant Material	Extraction Method (Solvent)	Optimum Condition	Optimum Yield, %	References
Gmelina Seed	Solvent extraction (n-hexane)	Extraction time = 60 mins, Volume of solvent = 150 ml, and Particle size = 0.15 mm	52.09	[18]
Jatropha curcas seed	Solvent extraction (n-hexane)	Extraction temperature = 69.67 ◦ C, Particle size = 0.63 mm, and Solvent/solid ratio = 9.98:1 ml/g	56.69	[7]
Pumpkin Seeds	Solvent extraction ethanol)	Temperature = 75°C, Extraction time = 270 mins and Particle size = 0.25 mm	56.20	[19]
Mahogany seed	Solvent extraction (n-hexane)	Particle size = 1 mm Extraction temperature = 68 °C Extraction time = 106 min Solvent/solid ratio = 5.05:1	58.9	This Study

The achieved yield of 58.9% is notably higher than that reported for Gmelina seed (52.09%) [18] under similar extraction conditions using n-hexane as the solvent. This suggests that, under optimised conditions, mahogany seeds can yield a more significant amount of oil than Gmelina seeds.

This study's optimised extraction time of 106 minutes, shorter than the 270 minutes used for Pumpkin seed extraction [19], it proved sufficient to achieve a high oil yield. This shorter extraction time indicates a more efficient process in terms of time and energy consumption.

Although the Pumpkin seed study [19] achieved a slightly higher yield (56.20%) using ethanol, using ethanol as a solvent introduces additional complexities regarding its higher boiling point, making solvent recovery more challenging. The chosen extraction temperature of 68 °C aligns with the optimal temperatures reported for Jatropha curcas (69.67 °C) [7] and falls within the range typically observed for efficient oil extraction. This moderate temperature likely enhances oil solubility and mass transfer rates without promoting thermal degradation of the oil. The solvent/solid ratio of 5.05:1 employed in this study effectively achieved a high oil yield while using a relatively lower amount of solvent compared to some studies. This efficient solvent usage is beneficial for economic and environmental reasons, as it reduces solvent consumption and the associated costs of solvent recovery and recycling. Using a smaller particle size (1 mm) further contributed to the efficient oil extraction. The smaller particle size provides a larger surface area for the solvent to interact with the seed material, facilitating the dissolution and extraction of the oil, consistent with observations in other studies.

Characterisation of the extracted oil. The optimum values of the four factors were used to prepare 1 l of mahogany oil, which was subjected to physicochemical determination and characterisation.

The physicochemical properties of the mahogany oil extracted in this study were compared to data reported in the literature (Table 6). These properties are crucial in determining the oil's suitability for biodiesel conversion and potential fuel quality.

Table 6 – Physicochemical properties of optimised mahogany oil

Parameter	This study	[5]	[16]	[17]
Moisture content (% w/w)	3	-	-	-
Density (kg/m^3) (30 °C)	915	962	898	917.3
Acid value (mg KOH/g oil)	7.99	-	15.71	-
Kinematic viscosity (mm^2/s at 30 °C)	20.99	-	21.98	-
Saponification value (mg KOH/g oil)	200.21	186	224.4	192.9
Calorific value (MJ)	36.55	-	-	-

The extracted mahogany oil's low moisture content (3% w/w) is favourable for biodiesel production. High moisture levels can hinder the transesterification reaction and lead to soap formation, reducing biodiesel quality [20]. The density of 915 kg/m^3 aligns well with the values reported by [17] (917.3 kg/m ^{3}) and [16] (898 kg/m ^{3}), suggesting consistency in the density of mahogany seed oil across different sources and extraction methods. The slightly higher value reported by [5] (962 kg/m ^{3}) might indicate variability in seed composition or extraction techniques. The acid value of 7.99 mg KOH/g is notably lower than the 15.71 mg KOH/g oil reported by [16]. A lower acid value is advantageous for biodiesel production as it reduces the need for extensive pretreatment to neutralise free fatty acids, which can cause engine corrosion issues. The kinematic viscosity of 20.99 mm^2/s is comparable to the value reported by [16] (21.98 mm^2/s), indicating similar flow properties. Viscosity is a crucial parameter for fuel injection and atomisation, and the values obtained suggest that the extracted mahogany oil possesses suitable viscosity characteristics for biodiesel conversion. The saponification value of 200.21 mg KOH/g oil aligns with the range reported in the literature (186-224.4 mg KOH/g oil). This suggests that our extracted mahogany oil's average fatty acid chain length is consistent with other studies. The saponification value provides insights into the amount of alkali required for complete transesterification during biodiesel production. The high calorific value of 36.55 MJ is a positive indicator for fuel applications, suggesting that biodiesel produced from this mahogany oil would have good energy content.

The fatty acid composition of the extracted mahogany oil was analysed using Gas Chromatography-Mass Spectrometry (GC-MS). The chromatogram in Figure 9 revealed a complex mixture of compounds, with significant peaks corresponding to fatty acid methyl esters (FAMEs), as expected for vegetable oil.

Table 6 presents the identified compounds and their relative abundance based on peak area percentages. The analysis confirmed that mahogany oil is rich in unsaturated fatty acids, with oleic acid (combined area of 24.43% for peaks 8 and 11) and linoleic acid (38.93% combined area for peaks 13, 14, and 15) being the most abundant. A significant amount of 2-chloroethyl linoleate (11.33%), a derivative of linoleic acid, was detected.

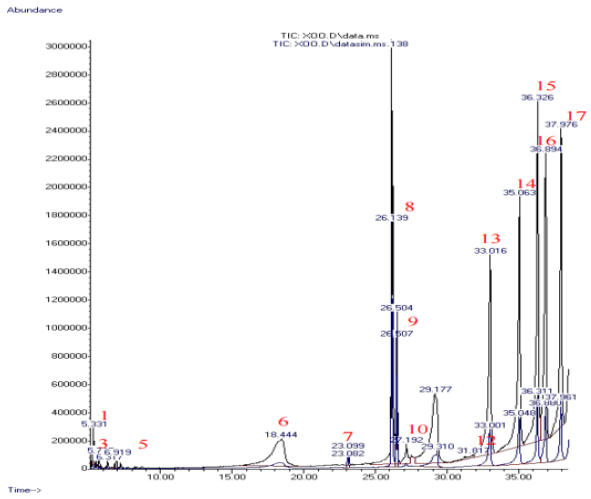

Figure 9 – The GC-MS Spectrogram of Mahogany Seeds Oil

Palmitic acid (0.34%) and stearic acid (2.74%) were also minor components. The high content of unsaturated fatty acids, particularly linoleic and oleic acids, is typical of many vegetable oils and can affect the properties of the biodiesel produced, such as its cold flow properties and oxidative stability [21]. This result is similar to that obtained by [17]. Both studies identified oleic acid, linoleic acid, palmitic acid, and stearic acid as significant components of mahagoni seed oil, with unsaturated fatty acids predominating. However, notable differences in relative proportions were observed. The current study showed higher percentages of linoleic acid (38.93%) compared to [17] (32.6%). In comparison, similar proportions of oleic acid were found in both studies (24.43% in this study and 25.5%) [17]. Additionally, this study reported lower percentages of palmitic and stearic acids (0.34% and 2.74%, respectively) than [17] (13.0% and 14.1%). Linolenic acid was reported by [17] (12.2%) but was not explicitly identified in the current GC-MS results.

In addition to the FAMEs, several other compounds were detected in smaller quantities. These include Toluene, due to impurities in the extraction solvent used, and various cyclohexanes and benzene derivatives, which are likely impurities. The presence of 9-Octadecenal (Oleic Aldehyde) and 9,17-Octadecadienal (Linoleic Aldehyde) could indicate some degree of oxidation of the unsaturated fatty acids during oil extraction or storage.

Table 6 – GC-MS Analysis of Extracted Mahogany Oil

Peak	RT	Area %	Library/ID	Similarly Index	General Name	Chemical Formula
1	5.3308	0.4212	Toluene	90	Toluene	$C_6H_5CH_3$
2	5.4535	0.2207	Cyclohexane, 1,3-dimethyl-, trans-	90	Cyclohexane, 1,3-dimethyl-, trans-	C_8H_{16}
3	5.7367	0.2014	Cyclohexane, 1,2-dimethyl-, cis-	70	Cyclohexane, 1,2-dimethyl-, cis-	C_8H_{16}
4	6.3169	0.1846	Cyclooctane, butyl-	59	Butylcyclooctane	$C_{12}H_{24}$
5	6.9192	0.3045	Benzene, 1,3-dimethyl-	94	m-Xylene	C_8H_{10}
6	18.4439	7.5043	12-Methyl-E,E-2,13-octadecadien-1-ol	89	Branched Fatty Alcohol	$C_{19}H_{36}O$
7	23.099	0.3418	Hexadecanoic acid	97	Palmitate acid	$C_{16}H_{32}O_2$
8	26.1385	13.9975	cis-9-Octadecenoic acid	99	Oleic acid	$C_{18}H_{34}O_2$
9	26.507	2.7405	Octadecanoic acid	98	Stearate acid	$C_{19}H_{38}O_2$
10	27.1919	1.1032	9-Octadecenal	58	Oleic aldehyde	$C_{18}H_{34}O$
11	29.1768	10.4282	cis-9-Octadecenoic acid	46	Oleic acid	$C_{18}H_{34}O_2$
12	31.8171	0.4699	9,17-Octadecadienal, (Z)-	90	Linoleic aldehyde	$C_{18}H_{32}O$
13	33.0157	11.6013	9,12-Octadecadienoic acid (Z,Z)-	91	Linoleic acid	$C_{18}H_{32}O_2$
14	35.0629	12.7418	9,12-Octadecadienoic acid (Z,Z)-	92	Linoleic acid	$C_{18}H_{32}O_2$
15	36.3255	14.5849	9,12-Octadecadienoic acid (Z,Z)-	86	Linoleic acid	$C_{18}H_{32}O_2$
16	36.8944	11.3336	2-Chloroethyl linoleate	89	2-Chloroethyl Linoleate	$C_{20}H_{35}ClO_2$
17	37.9759	11.8205	9,17-Octadecadienal, (Z)-	83	Linoleic aldehyde	$C_{18}H_{32}O$

Fourier-transform infrared spectroscopy (FTIR) analysis was performed to characterise the functional groups in the extracted mahogany oil. The FTIR spectrum (Figure 10) exhibited characteristic peaks associated with triglycerides and fatty acids.

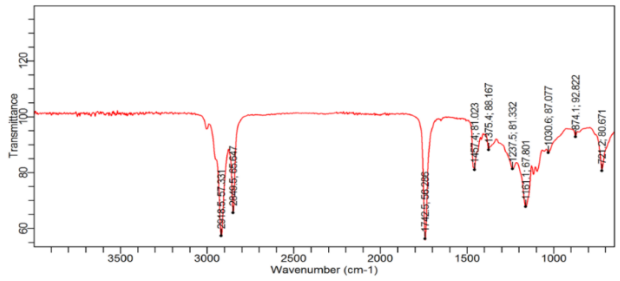

Figure 10 – Fourier Transform Infra-Red (FTIR) Spectra of Mahogany Seed Oil

A prominent peak at 1742 cm^{-1} was assigned to the C=O stretching vibration of ester groups, confirming the presence of triglycerides in the oil. Firm peaks at 2918 - 2849 cm^{-1} were attributed to C-H stretching vibrations, indicating the presence of long hydrocarbon chains, characteristic of fatty acids.

The characteristic peaks in the FTIR spectrum were analysed and assigned to their corresponding functional groups based on standard FTIR correlation charts [22]. The FTIR spectrum of the mahogany seed oil extracted in this study (Figure 10) showed strong similarities to that reported by [6] for mahogany seed oil. Both spectra exhibited characteristic peaks associated with aliphatic hydrocarbons (C-H stretches at 2924 cm^{-1} and 2854 cm^{-1}), ester groups (C=O stretch at 1743 cm^{-1}), and methyl groups (CH_3 bend at 1373 cm^{-1}).

Process Simulation and Solvent Recovery. An Aspen Plus® model was developed to simulate the entire extraction process, including purification and solvent recovery. Sensitivity analyses were performed on the distillation column, varying the number of stages and reflux ratio to minimise hexane content in the final oil product. With 25 stages and a reflux ratio of 0.155, the optimised model achieved 99.99% oil purity and 100 % hexane recovery. This demonstrates the potential of combining experimental optimisation with process simulation for achieving efficient and sustainable biodiesel production from non-edible seed oils.

Figure 11 depicts the behaviour of the solvent on the oil yield based on the Aspen Plus® model, where an increase in the solvent flow produces an increase in the oil yield within the region of 1:5 for the solid-to-solvent ratio set. In this case, the oil is represented by the combination of fatty acids.

In modelling the distillation column (DST from Figure 1), the initial number of stages and reflux ratio assumed was 15 and 3, respectively, to obtain the desired separation. Still, a substantial number of hexanes remained in the oil stream. To get the desired separation (with little or no hexane in the oil) or the optimum values of these parameters, a sensitivity analysis was performed in Aspen Plus to investigate the effect of the number of distillation stages on hexane recovery efficiency.

As shown in Figure 12, the hexane flow rate in the distillate stream decreased sharply as the number of stages increased from 14 to 25, indicating a significant improvement in hexane separation from the biodiesel and glycerol. However, beyond 25 stages, the change in hexane flow rate remains the same with an increase in the number of stages. Based on this analysis, a distillation column with 25 stages was optimal for the process, balancing hexane recovery efficiency with equipment cost and energy consumption.

Figure 13 presents the predicted flow rate of hexane in the distillate stream as a function of the reflux ratio. The simulation employed the NRTL thermodynamic model and assumed a feed composition consistent with the experimentally obtained product mixture.

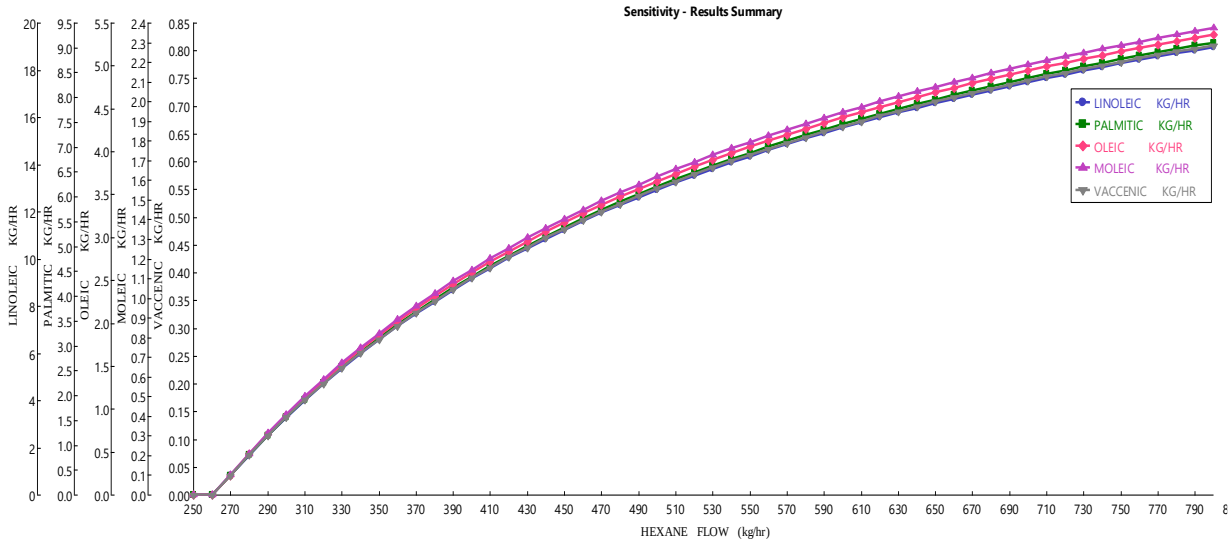

Figure 11 – Solvent Sensitivity Analysis Against the Oil Yield (based on Figure 1)

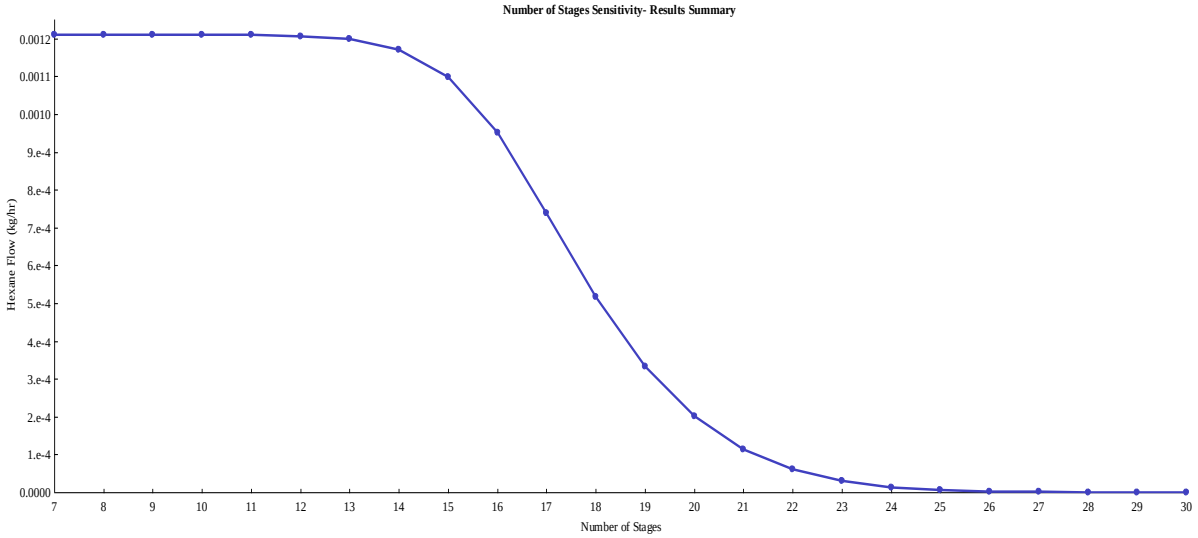

Figure 12 – Sensitivity analysis of hexane flow rate versus the number of distillation stages (based on Figure 1)

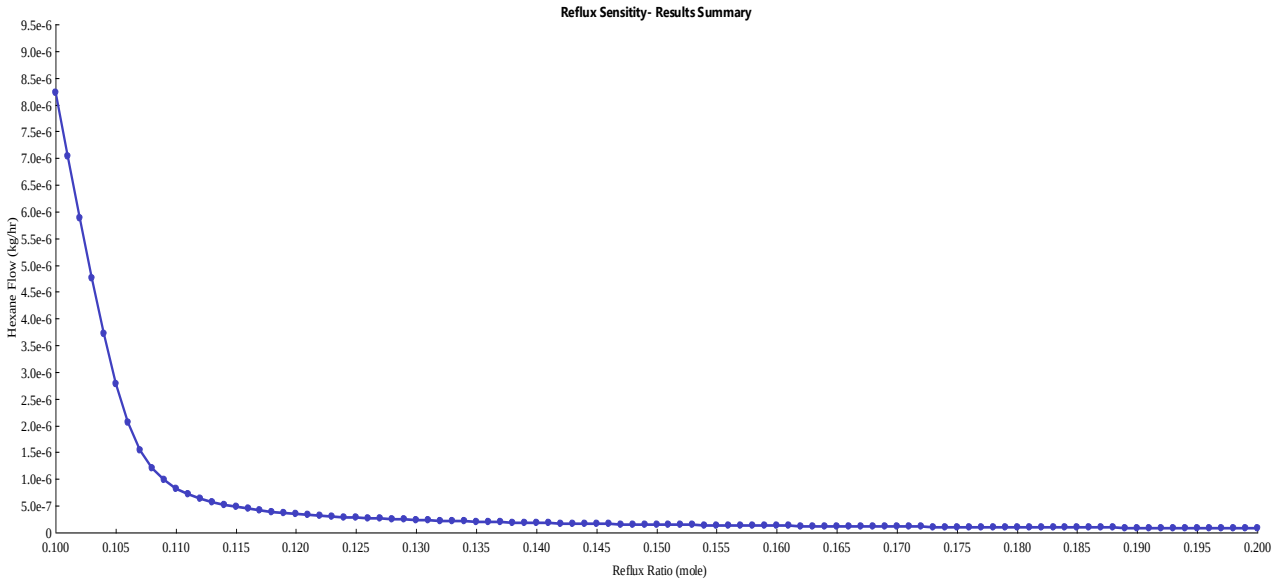

Figure 13 – Sensitivity analysis of hexane flow rate in the distillate stream as a function of reflux ratio (based on Figure 1)

As illustrated in Figure 13, increasing the reflux ratio initially leads to a steep decline in the hexane flow rate exiting the top of the distillation column. The reflux ratio, defined as the ratio of condensed liquid returned to the column (reflux) to the liquid collected as distillate, is crucial in controlling separation efficiency within the column. A higher reflux ratio generally results in a purer distillate stream. In this case, the sharp decrease in hexane flow rate suggests that increasing the reflux ratio to approximately 0.12 significantly improves the separation of hexane from the biodiesel and glycerol components. However, beyond a reflux ratio of 0.12, the hexane flow rate plateaus, with only marginal reductions observed despite further increases in the reflux ratio. This indicates diminishing returns in terms of hexane purity beyond this point. While a higher reflux ratio theoretically leads to better separation, it also comes at the cost of increased energy consumption, as more energy is required to vaporise and condense the refluxed liquid.

This sensitivity analysis selected a reflux ratio of 0.12 as the optimal value for the biodiesel purification process. This value balances the need for high hexane recovery with minimising energy consumption in the distillation column. This optimisation strategy contributes to a more economically viable process and aligns with green chemistry principles by reducing energy usage and promoting efficient solvent recovery.

Table 7 shows the predicted mass flow rates of critical components in the separation module (Figure 1) based on the optimised reaction conditions determined experimentally.

Table 7 – Optimise Flow of the components in the Separation Module

	(kg/hr)							
	Input				Output			fraction
Component	S7	Extract	S8	S9	Cake	Sol-Rec	Oil	Oil
H_2O	0.866	0	0	0	0.866	0	0	0
Seed	39.543	0	0	0	39.543	0	0	0
Palmitic acid	5.691	9.705	5.634	15.339	0.057	0.000	8.057	0.1450
Oleic acid	2.989	5.097	2.959	8.057	0.030	0.000	15.339	0.2761
Linoleic acid	10.472	17.856	10.367	28.223	0.105	0.000	28.223	0.5081
Oleic derivative	0.959	1.634	0.949	2.583	0.010	0.000	2.583	0.0465
N-HEXANE	295.733	504.267	292.776	797.043	2.957	797.035	0.008	0.0001
Stearate acid	0.497	0.847	0.492	1.339	0.005	0.000	1.339	0.0241
Total	356.750	539.406	313.178	852.584	43.572	797.035	55.550	1.0000

S7 represents the cake of the seed, containing residual n-hexane and traces of oil. "Extract" refers to the extracted oil and hexane mixture. S8 and S9 are intermediary streams within the separation process. "Sol-Rec" represents the recovered n-hexane stream, and "Oil" is the final purified oil stream. The Aspen Plus simulation indicates a remarkable n-hexane recovery rate exceeding 99.99%, as evidenced by the "Sol-Rec" stream. This high recovery rate is crucial for economic and environmental reasons, reducing the need for fresh solvents and minimising waste.

The "Oil" stream demonstrates successful oil extraction and purification. It primarily consists of fatty acids, with linoleic acid (50.81% by mass) being the most abundant, followed by oleic acid (27.61%) and palmitic acid (14.50%). The near-complete absence of water (H_2O) in the "Oil" stream confirms the effectiveness of the separation module in removing these components from the initial seed cake (S7).

This simulation provides valuable evidence for the scalability and efficiency of the oil extraction and purification process. The high solvent recovery and producing a purified oil stream rich in fatty acids support the potential for sustainable and economically viable biodiesel production from mahogany seeds.

CONCLUSIONS

The ANOVA result showed that the model adequately represented the extraction system with a p-value of 0.0001 and an F-value of 29.81. The optimum conditions of extraction were found to be 103.8 minutes of extraction time, a temperature of 68°C, a solvent/solid ratio of 5.05, and a particle size of 1 mm. The maximum yield of the oil obtained experimentally under these conditions was 58.9 %, which is well compared with the predicted value of 61.6%.

The extracted mahogany oil exhibited physicochemical properties suitable for biodiesel conversion. Low moisture content (3%) and a moderate acid value (7.99 mg KOH/g oil) suggest minimal pretreatment requirements. Density, viscosity, and saponification values align with the literature, indicating compatibility with conventional biodiesel processing methods. The high calorific value promises good energy content for the resulting biodiesel.

GC-MS analysis confirmed the oil's richness in unsaturated fatty acids, predominantly linoleic acid (38.93%), oleic acid (24.42%) and a small amount of saturated fatty acids; Palmitic (0.34%) and stearic (2.74%). However, the presence of a significant amount of 2-chloroethyl linoleate, a derivative of linoleic acid, warrants further investigation to understand its potential influence on biodiesel properties.

An Aspen Plus simulation of the extraction process, incorporating a distillation unit for solvent recovery, predicted a near-complete hexane recovery rate (99.99%), highlighting the potential for a highly efficient and environmentally friendly industrial-scale process.

REFERENCES

1. Salih, N., & Yahia, E. (2015). *Khaya Senegalensis* seed: Chemical characterisation and potential uses. *Journal of Chemical and Pharmaceutical Research, 7*(6), 409–415.

2. Ibrahim, H., Fasanya, O. O., Hayatudeen, A., & Osa-Benedict, E. O. (2018). Fatty Acid Composition of Mahogany Seed Oil and its Suitability for Biodiesel Production. *Nigerian Journal of Technological Research, 13*(1), 45. doi: 10.4314/njtr.v13i1.4

3. Nguyen, N.-V. T., Nguyen, C. V., Duong, N. T., Dai, X.-T. T., Nguyen, K. T., & Le, C.-T. T. (2024). Optimisation of ultrasound-assisted extraction using response surface methodology and quantification of polyphenol compounds in Avicennia officinalis L. from Vietnam. *Pharmacia, 71*, 1–9. doi: 10.3897/pharmacia.71.e115528

4. Abdurakhman, Y. B., Putra, Z. A., & Bilad, M. R. (2017). Aspen HYSYS Simulation for Biodiesel Production from Waste Cooking Oil using Membrane Reactor. *IOP Conference Series: Materials Science and Engineering, 180*, 012273. doi: 10.1088/1757-899x/180/1/012273

5. Okieimen, F. E., & Eromosele, C. O. (1999). Fatty acid composition of the seed oil of *Khaya Senegalensis*. *Bioresource Technology, 69*(3), 279–280. doi: 10.1016/s0960-8524(98)00190-4

6. Mursiti, S., Fitriani Rahayu, E., Maylia Rosanti, Y., & Nurjaya, I. (2019). Mahogany seeds oil: isolation and characterisations. *IOP Conference Series: Materials Science and Engineering, 509*, 012137. doi: 10.1088/1757-899x/509/1/012137

7. Yusuff, A. S. (2021). Parametric optimisation of solvent extraction of Jatropha curcas seed oil using design of experiment and its quality characterisation. *South African Journal of Chemical Engineering, 35*, 60–68. doi: 10.1016/j.sajce.2020.11.006

8. Bhattacharya, S. (2021). Central Composite Design for Response Surface Methodology and Its Application in Pharmacy. *Response Surface Methodology in Engineering Science*. doi: 10.5772/intechopen.95835

9. Jensen, W. A. (2014). Design and Analysis of Experiments by Douglas Montgomery: A Supplement for Using JMP®. *Journal of Quality Technology, 46*(2), 181–181. doi: 10.1080/00224065.2014.11917962

10. Jiyane, P. C., Tumba, K., & Musonge, P. (2018). Optimisation of <i>Croton gratissimus</i> Oil Extraction by <i>n</i>-Hexane and Ethyl Acetate Using Response Surface Methodology. *Journal of Oleo Science, 67*(4), 369–377. doi: 10.5650/jos.ess17197

11. AOCS. (2017). *Official Method Ca 2c-25*. Retrieved from https://myaccount.aocs.org/PersonifyEbusiness/Store/Product-Details?productId=111474

12. Wealleans, D. (2017). International Standards. *The Organizational Measurement Manual*, 139–149. doi: 10.4324/9781315554938-11

13. Dagde, K. K. (2019). Extraction of Vegetable Oil from Avocado Seed for the Production of Biodiesel (Alkyl Ester). *Journal of Natural Sciences Research*. doi: 10.7176/jnsr/9-3-01

14. Drews, A. (n.d.). Standard Test Method for Kinematic Viscosity of Transparent and Opaque Liquids (the Calculation of Dynamic Viscosity). *Manual on Hydrocarbon Analysis*, 6th Edition, 126-126–128. doi: 10.1520/mnl10842m

15. ASTM International. (2018). Test Method for Acid Number of Petroleum Products by Potentiometric Titration. doi: 10.1520/d0664-18e02

16. Olagbende, O. H., Falowo, O. A., Latinwo, L. M., & Betiku, E. (2021). Esterification of *Khaya Senegalensis* seed oil with a solid heterogeneous acid catalyst: Modeling, optimisation, kinetic and thermodynamic studies. *Cleaner Engineering and Technology, 4*, 100200. doi: 10.1016/j.clet.2021.100200

17. Mohan, M. R., Jala, R. C. R., Kaki, S. S., Prasad, R. B. N., & Rao, B. V. S. K. (2016). Swietenia mahagoni seed oil: A new source for biodiesel production. *Industrial Crops and Products, 90*, 28–31. doi: 10.1016/j.indcrop.2016.06.010

18. Ogbeide, S., Aniekwe, E., & Nwanno, C. (2018). Optimisation of the Extraction Process of Gmelina Seed Oil using Response Surface. *Chemistry Research Journal, 3*(5), 94–102.

19. Redrouthu, R., Sundramurthy, V. P., & Zergu, B. (2020). Extraction of Essential Oils from Pumpkin Seeds RSM Based Process Modeling, Optimization and Oil Characterization. International Journal of Engineering and Advanced Technology, 9(4), 1787–1797. doi: 10.35940/ijeat.d8420.049420

20. Chanakaewsomboon, I., & Moollakorn, A. (2021). Soap formation in biodiesel production: effect of water content on saponification reaction. *International Journal of Chemical and Environmental Sciences, 2*(2), 28–36. doi: 10.15864/ijcaes.2203

21. Alan C Hansen, & Bingjun Brian He. (2008). Food versus Fuel Characteristics of Vegetable Oils and Animal Fats. *2008 Providence, Rhode Island, June 29 - July 2*, 2008. doi: 10.13031/2013.25154

22. Wong, K. C. (2015). Review of Spectrometric Identification of Organic Compounds, 8th Edition. *Journal of Chemical Education, 92*(10), 1602–1603. doi: 10.1021/acs.jchemed.5b00571